Electronic Supplementary Information

An integrated electrochromic supercapacitor based on nanostructured Er-containing titania using a Er(III)-doped polyoxotitanate cage

Yaokang Lv,[a,c,d] Weishi Du,[a] Yan Ren,[a] Zhiwei Cai,[a] Cheng Zhang[a,*] Zuofeng Chen[b,*] and Dominic S. Wright[c,*]

College of Chemical Engineering and Materials Science, Zhejiang University of Technology, Hangzhou 310014, China. E-mail: czhang@zjut.edu.cn;

Department of Chemistry, Tongji University, Shanghai 200092, China. E-mail: zfchen@tongji.edu.cn;

Department of Chemistry, University of Cambridge, Lensfield Road, Cambridge CB2 1EW, UK. E-mail: dsw1000@cam.ac.uk;

Department of Chemistry, Tsinghua University, Beijing 100084, China;

Experimental Section

All chemicals were purchased from commercial sources and used as received, unless otherwise stated. Strict inert atmospheric conditions (dry and O_2-free) were employed throughout all synthetic and handling procedures [i.e., vacuum-line and using a glove box (M. Braun Labstar)]. IR spectra were recorded using a Nicolet 6700 spectrometer (Thermo Fisher Nicolet, USA) with KBr pellets. Both carbon and hydrogen analyses were carried out using a varioMicro Elemental analyzer (Elementar Analysensysteme GmbH, Germany). Powder X-ray diffraction (XRD) experiments were performed using a X'Pert Pro diffractometer with Cu-Kα radiation (λ= 1.5418Å) operating at 40 kV and 40 mA and the scanning angle ranged from 10 ° to 90° of 2θ. Scanning electron microscopy (SEM) images were collected using a field emission scanning electron microscope (Hitachi S-4800). Transmission electron microscopy (TEM) was performed with a FEI Tecnai G2 F30 electron microscope operating at an accelerating voltage of 300 kV. The surface compositions of sample **Er@TiO_2-A** and **Er@TiO_2-B** were determined by energy dispersive spectroscopy (EDS). EDS data were collected using an Thermo SCIENTIFIC energy dispersive X-ray spectroscopy system attached to a Hitachi S-4800 SEM, with an acceleration voltage of 15keV. X-ray photoelectron spectra (XPS) were operated on a spectrometer (Kratos AXIS Ultra DLD, Shimadzu, Japan). Thermal gravimetric analysis (TGA) was performed on a TGA Q5000 from TA Instruments.

*Synthesis and Characterisation of **1***

Titanium ethoxide (> 97% Sigma-Aldrich, 3.5 ml, 15.4 mmol), $ErCl_3$ (99% Sigma-Aldrich, 0.274g, 1mmol) and anhydrous ethanol (Sigma-Aldrich, 5.0ml) were mixed in a Teflon-lined autoclave and heated at 150 ^oC for 3 days. Slow cooling to room temperature gave a pink solution. Pink block crystals of $ErTi_8O_7(OEt)_{21}$ (**1**) were obtained by further evaporation of the solution at room temperature for about four weeks, yield 0.23 g (14.3 % with respect to Er supplied). Elemental analysis found C 31.2, H 6.5; cald. for **1**, C 31.4, H. 6.6. IR (800-4000 cm^{-1}), ν/cm^{-1} = 893.8(m), 920.6(m), 1051.7(vs), 1070.3(vs), 1147.5(vs), 1354.5(w), 1375.2(m), 1440.7(w), 2361(w), 2695.5(w), 2858.2(m), 2923.1(m), 2968.0(m), 3382.5(w).

Single Crystal X-ray Crystallography

Crystal data were collected on a Bruker Smart Apex CCD diffractometer using Mo(Kα) radiation (λ = 0.71073 Å). The structures were solved by Direct Methods and refined by full-matrix least squares on F^2. (Ref: SHELX, G. M. Sheldrick, *Acta Crystallogr.* 2008, **A64**, 112). The hydrogen atoms were introduced to calculate positions and refine with fixed geometry with respect to their C atoms. The data and refinement are summarized and shown in Table **S1**. Selected bond lengths (Å) and angles (^{o}) are shown in Table **S2**.

Table S1. Details of the structure solution and refinement of **1.**

Compound	**1**
Chemical formula	$\mathbf{C_{42}H_{105}ErO_{28}Ti_8}$
FW	1608.72
Crystal system	Triclinic
Space group	*P-1*
Unit cell dimensions	3547.8(5)
a (Å)	12.7613(11)
b (Å)	13.6635(12)
c (Å)	22.0141(17)
α (°)	98.633(3)
β (°)	95.552(3)
γ (°)	108.856(2)
V (Å^3)	1796.3(2)
Z	2
ρ_{calc} (Mg/m^3)	1.506
μ (Mo-Kα) (mm^{-1})	2.088
Goodness-of-fit on F_2	1.017
reflections collected	33108
independent reflections (R_{int})	12374 (0.046)
*R*1, *wR*2 [$I>2\sigma(I)$]	0.0519, 0.1332
*R*1, *wR*2 (all data)	0.0757, 0.1512

Table S2. Selected bond lengths (Å) and angles (°).

Bond	Distance	Bond	Distance
Er1—O3	2.305(4)	Er1—O2	2.345(5)
Er1—O1	2.311(4)	Er1—O8	2.352(4)
Er1—O4	2.339(5)	Er1—O5	2.356(4)
Er1—O6	2.345(4)	Er1—O7	2.364(5)
O3—Er1—O1	148.51(17)	O3—Er1—O8	131.90(17)
O3—Er1—O4	68.11(16)	O1—Er1—O8	70.52(16)
O1—Er1—O4	97.06(16)	O4—Er1—O8	85.12(16)
O3—Er1—O6	70.46(16)	O6—Er1—O8	104.14(16)
O1—Er1—O6	131.87(16)	O2—Er1—O8	130.90(16)
O4—Er1—O6	130.77(16)	O3—Er1—O5	137.40(16)
O3—Er1—O2	96.92(17)	O1—Er1—O5	65.03(16)
O1—Er1—O2	68.03(16)	O4—Er1—O5	152.77(16)
O4—Er1—O2	124.72(17)	O6—Er1—O5	68.35(15)
O6—Er1—O2	85.30(17)	O2—Er1—O5	69.51(16)
O8—Er1—O5	69.91(16)	O6—Er1—O7	69.97(16)
O3—Er1—O7	65.08(16)	O2—Er1—O7	152.92(16)
O1—Er1—O7	137.41(16)	O8—Er1—O7	68.31(15)

O4—Er1—O7	69.25(16)	O5—Er1—O7	109.19(16)

Fig. S1. 0.01 mol/L dichloromethane (DCM) solution of **1**.

Preparation of ***Er@TiO$_2$-A*** *and* ***Er@TiO$_2$-B***

Dried crystals of **1** was sintered at 500 ℃ for 10 hour in a dry air flow, pink solids of Er(III)-doped TiO_2 was obtained, named **Er@TiO$_2$-A.**

A 0.01 mol/L dichloromethane (DCM) solution of **1** were sprayed via 0.3 mm diameter airbrush and dried at room temperature. The obtained power was further sintered at 500 ℃ for 10 hour in air flow and pink-white powder of Er(III)-doped TiO_2 was obtained, named **Er@TiO$_2$-B**.

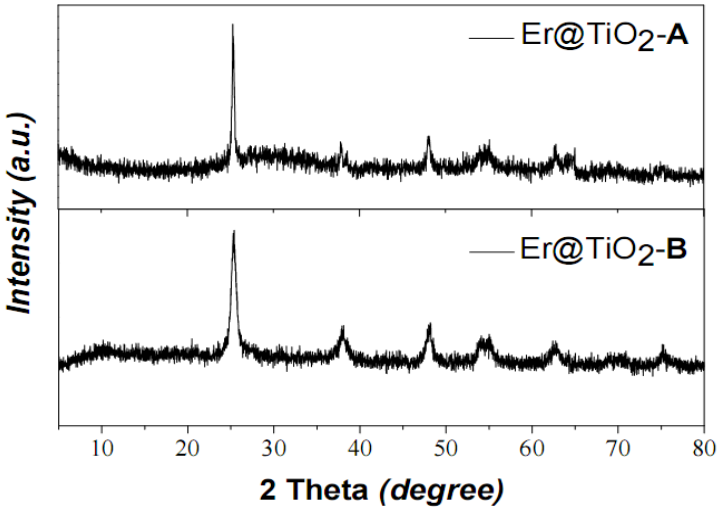

Fig. S2. Powder XRD results of **Er@TiO$_2$-A** and **Er@TiO$_2$-B**. The diffraction peaks at 2θ = 25.29^o, 37.81^o, 48.05^o, 55.07^o and 62.70^o can be indexed to (1,0,1), (0,0,4), (2,0,0), (2,1,1) and (2,0,4) crystal planes of **1**, which denote anatase TiO_2 (JCPDS 21-1272).

As shown in Fig. S2, the broadening of the peak at full width half maximum is related to the average diameter (D) of the particles according to Debye–Scherrer's equation (Ref: L. S. Birks and H. Friedman, *J. Appl. Phys.* 1946, **17**, 687), i.e. $D = 0.9\lambda / B \cos\theta$, where λ is X-ray wavelength, B is line broadening measured at half height and θ is Bragg angle. The average crystalline sizes are obtained from most predominant peak, corresponding to (1 0 1) reflection. The calculated average crystalline size of **Er@TiO_2-A** is 26.84nm, which is larger than that of **Er@TiO_2-B** (11.50nm).

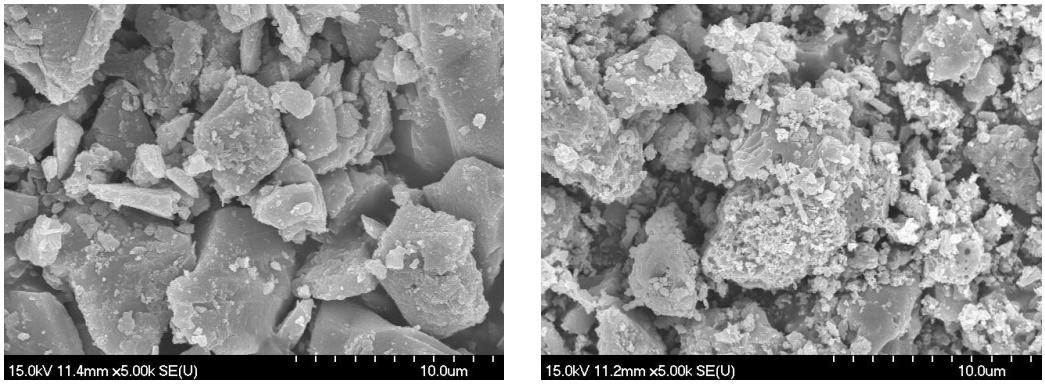

(a) **(b)**

Fig. S3. (a) SEM image of **Er@TiO_2-A**, (b) SEM image of **Er@TiO_2-B**.

*XPS Analysis of **Er@TiO_2-A** and **Er@TiO_2-B***

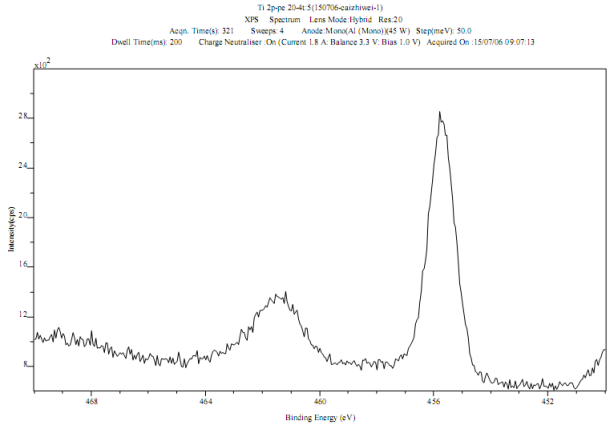

Fig. S4. XPS signal of **Er@TiO_2-A** for Ti *2p* region.

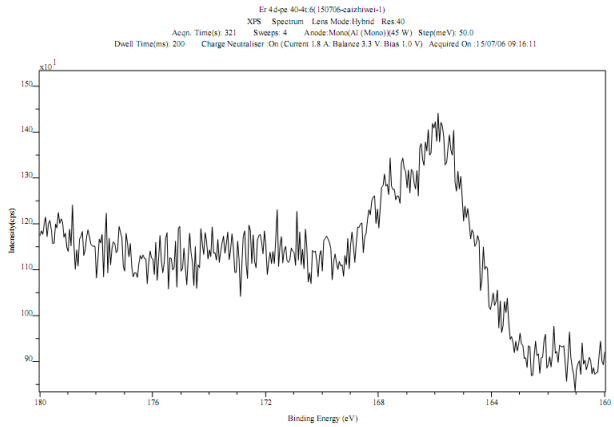

Fig. S5. XPS signal of **Er@TiO$_2$-A** for Er 4*d* region.

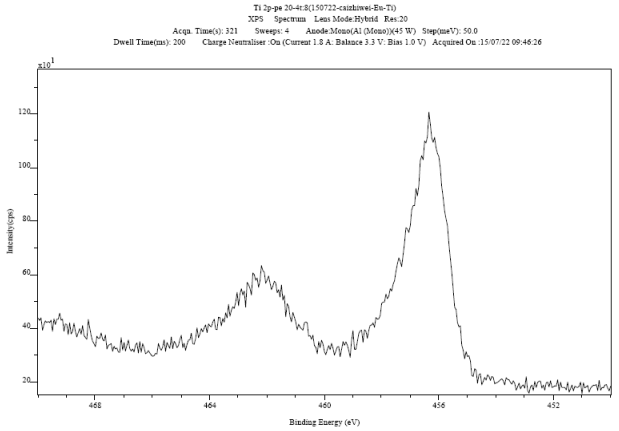

Fig. S6. XPS signal of **Er@TiO$_2$-B** for Ti *2p* region.

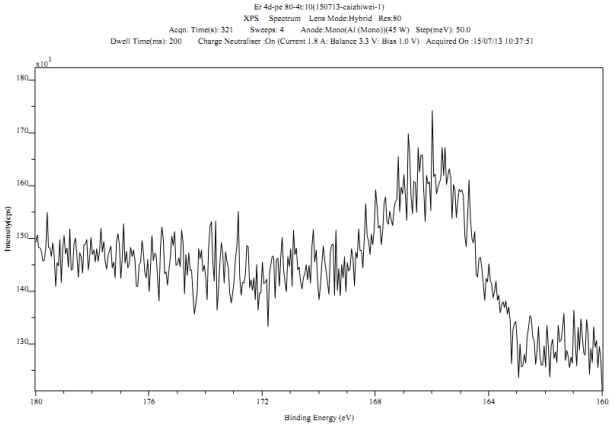

Fig. S7. XPS signal of **Er@TiO$_2$-B** for Er 4*d* region.

EDS Analysis of ***Er@TiO$_2$-A*** *and* ***Er@TiO$_2$-B***

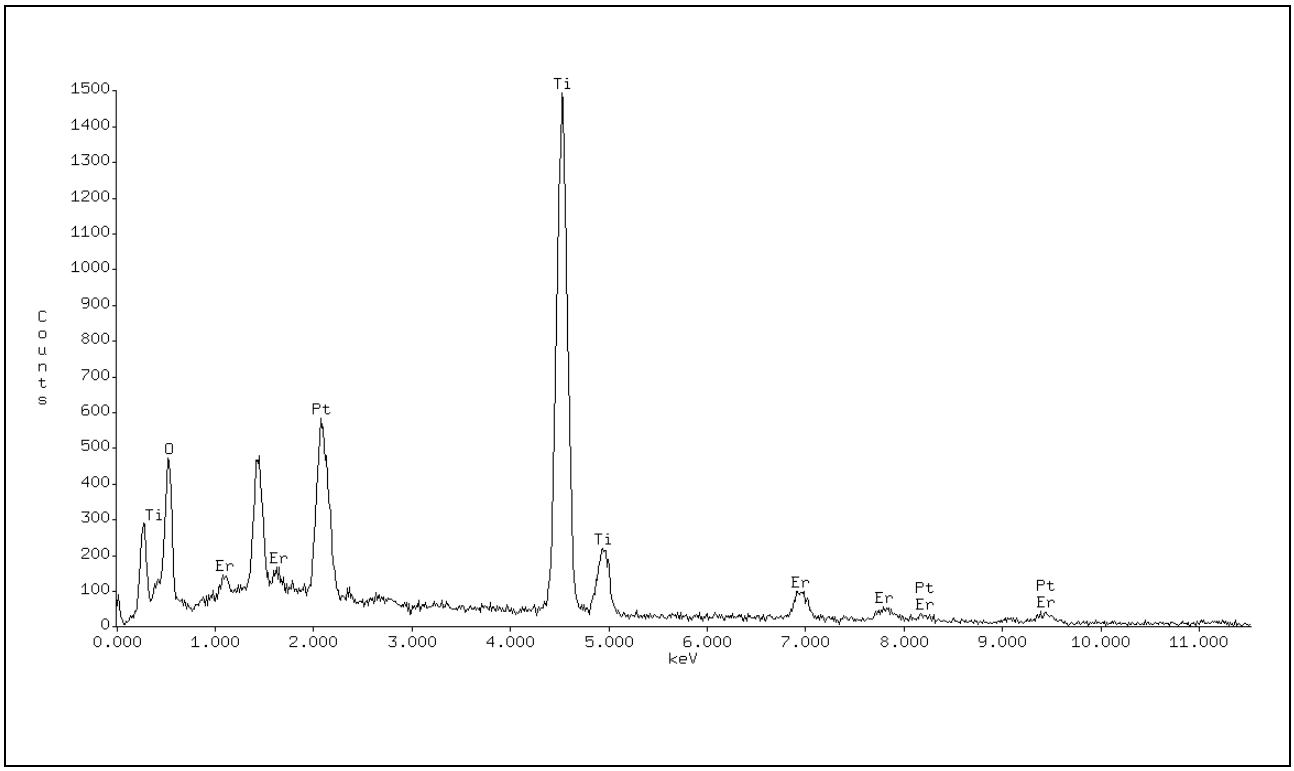

Fig. S8. EDS of **Er@TiO$_2$-A.**

Table S3. EDS of **Er@TiO$_2$-A.**

Quantitative Analysis

PROZA Correction Acc.Volt.= 15 kV Take-off Angle=29.33 deg

Number of Iterations = 5

Element	k-ratio (calc.)	ZAF	Atom %	Element Wt %	Wt % Err. (1-Sigma)	No. of Cations
O -K	0.0512	4.893	62.53	25.04	+/- 0.47	---
Ti-K	0.3238	1.061	28.65	34.36	+/- 0.36	10.997
Er-L	0.1123	1.302	3.49	14.63	+/- 1.31	1.341
Pt-L	0.1848	1.405	5.32	25.97	+/- 4.59	2.041
Total			100.00	100.00		14.379

The number of cation results are based upon 24 Oxygen atoms

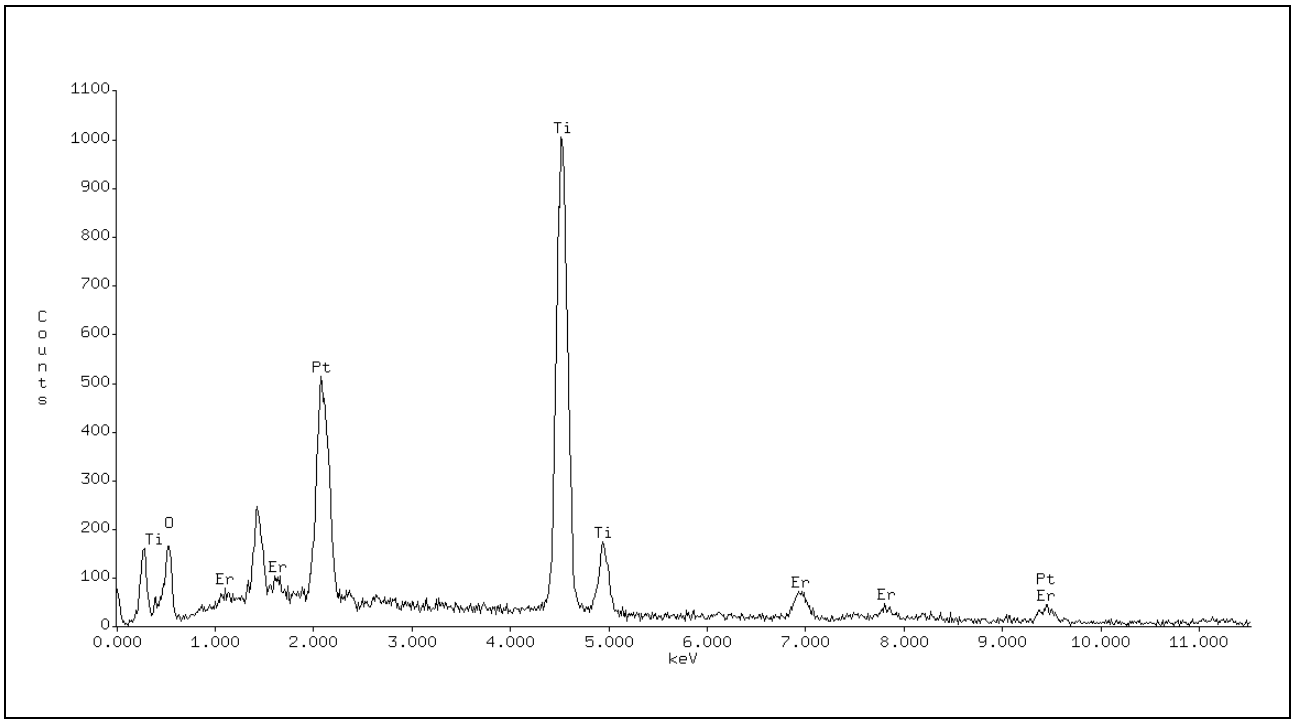

Fig. S9. EDS of **Er@TiO_2-B.**

Table S4. EDS of **Er@TiO_2-B.**

Quantitative Analysis

PROZA Correction Acc.Volt.= 15 kV Take-off Angle=29.33 deg

Number of Iterations = 5

Element	k-ratio (calc.)	ZAF	Atom %	Element Wt %	Wt % Err. (1-Sigma)	No. of Cations
O -K	0.0298	5.001	48.54	14.89	+/- 0.43	---
Ti-K	0.3310	1.031	37.18	34.14	+/- 0.44	18.381
Er-L	0.1197	1.228	4.58	14.70	+/- 1.61	2.266
Pt-L	0.2773	1.308	9.70	36.28	+/- 3.85	4.796
Total			100.00	100.00		25.444

The number of cation results are based upon 24 Oxygen atoms

Electrode preparation and cell assembling

Anatase nanoparticles (CAS no. 13463-67-7), purchased from aladdin industries corporation, were used as the control group for evaluating the lithium ion storage properties of **Er@TiO_2-A** and **Er@TiO_2-B**.

The working electrodes for electrochemical measurements were prepared by mixing the active material (**Er@TiO_2-A**, **Er@TiO_2-B** as well as anatase nanoparticles), polyvinylidene fluoride and carbon black with a weight ratio of 8:1:1 in N-methylpyrrolidone and then equably coated on the copper foil. After that, the electrode film was dried at 100 ^{o}C for 12 h and cut into discs with a diameter of 12 mm. The cycling cells were assembled by using **Er@TiO_2-A** or **Er@TiO_2-B** or anatase disc as working electrode, metal lithium foil as counter electrode, porous polypropylene fiber as separator and 1 mol/L $LiPF_6$ dissolved in a mixture of ethylene carbonate and dimethyl carbonate (1:1, v/v) as electrolyte. All the cells were assembled in an argon-filled glove box, where both moisture and oxygen levels were kept at less than 1 ppm.

Electrochemical analysis

Galvanostatic charge/discharge experiments and rate performance of cells were measured on a multi-channel Land battery testing system at room temperature. Cyclic voltammograms (CVs) and electrochemical impedance spectroscopy (EIS) analysis were recorded on a CHI 660E electrochemical workstation at room temperature. China). The optical contrast and switching time of the composite film are carried out on a Shimadzu UV-1800 UV–vis spectrophotometer (Shimadzu, Japan).

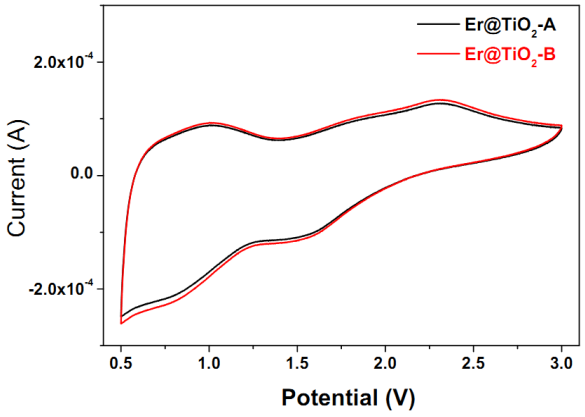

Fig. S10. CV curves (Voltage v.s. Li/Li^+) of **Er@TiO_2-A** and **Er@TiO_2-B** at a scan rate of 2.0 mV s^{-1}.

Preparation of ***Er@TiO$_2$-B*** *films*

Thin films of **Er@TiO$_2$-B** were spray-cast onto indium tin oxide (ITO) coated glass slides from 0.1 mol/L DCM solution of **1,** and sintered at 500 ℃ afterwards.

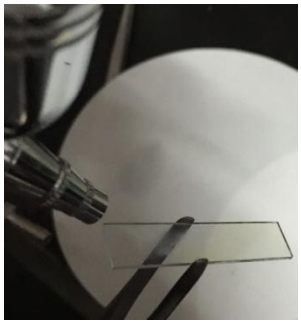

Fig. S11. Image of DCM solution of **1** spray-cast onto an ITO coated glass slide.

(a) (b)

Fig. S12. bleached state (a) and colored state (b) of the **Er@TiO$_2$-B** film.

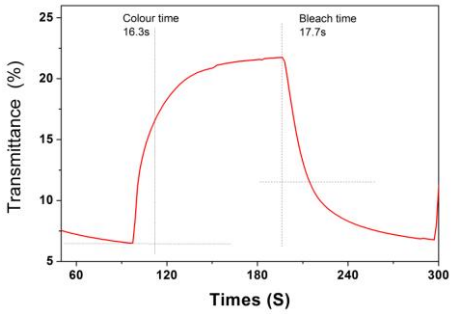

Fig. S13. Electrochromic switching response of **Er@TiO$_2$-B** film.

As shown in Fig. S13, the color-switching time of **Er@TiO_2-B** film was estimated as the time taken for the absorbance to change by two-thirds of the difference between the steady-state absorbance in the colored and bleached states. The switching time was 16.3 s for coloration and 17.7 s for bleaching.

Preparation of the PTBTPA film

The poly(4,4',4"-tris[4-(2-bithienyl)pheny]amine) (**PTBTPA**) film was prepared via electro-polymerization on the ITO glass substrate. The electro-polymerization route is similar with that described previously[13b] As shown in **Scheme S1**, the **PTBTPA** film was obtained via the constant potential polymerization of 0.75 mmol/L 4,4',4"-tris[4-(2-bithienyl) pheny]amine (**TBTPA**) and 0.1 mol/L tetrabutylammonium perchlorate (TBAP) in DCM/acetonitrile (ACN) solutions (7 : 3, by volume) at 1.2 V, which was performed in a conventional three compartment electrolysis cell with ITO substrate (the active area: 2.9 cm × 2.6 cm) as the working electrode, a platinum (Pt) sheet (4 cm^2) as the counter electrode and a double-junction Ag/AgCl electrode (silver wire coated with AgCl in saturated KCl solution, 0.1 M TBAP in DCM/ACN solution as the second junction) as the reference electrode. The charge capacity of polymerization was controlled at 4×10^{-2} C.

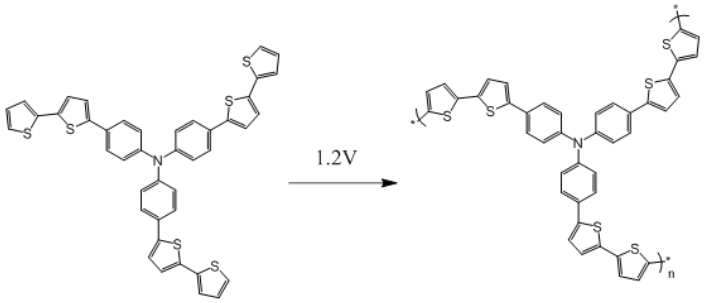

Scheme S1. Electro-polymerization route for **PTBPTA**.

Preparation of $LiClO_4$-PMMA gel

The high viscosity gel electrolyte ($LiClO_4$-PMMA gel) based on poly(methyl methacrylate) (PMMA) and lithium perchlorate ($LiClO_4$) was plasticized by propylene carbonate to form a highly conducting and transparent gel. To ease the gel synthesis, the PMMA and $LiClO_4$ were first dissolved in acetonitrile (ACN). The composition of the casting solution was $LiClO_4$/PMMA/PC/ACN in a ratio of 3:7:20:70 by weight.

(see Ref: I. Schwendeman, J. Hwang, D. M. Welsh, D. B. Tanner and J. R. Reynolds, *Adv. Mater.* 2001, **13**, 634-637.)

Integration of electrochromic supercapacitor

A sandwich-like EC supercapacitor was assembled by stacking a **Er@TiO_2-B** film and a **PTBTPA** film with $LiClO_4$-PMMA (PMMA is polymethyl methacrylate) gel as electrolyte.

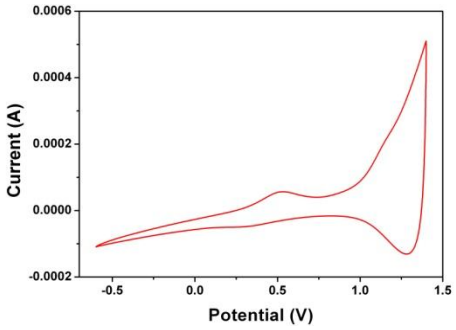

Fig. S14. CV curve of an as-prepared EC supercapacitor at a scan rate of 50 mV s^{-1}.

CV curve of the EC supercapacitor exhibit two pairs of redox peaks around 0.5 V and 1.3 V, corresponding to ion insertion and extraction reactions in the electrode films.

Table S5. Table of areal capacitance at different current densities.

current density (mA/cm^2)	areal capacitance (F/cm^2)
0.5	0.020
0.75	0.018
1.0	0.016

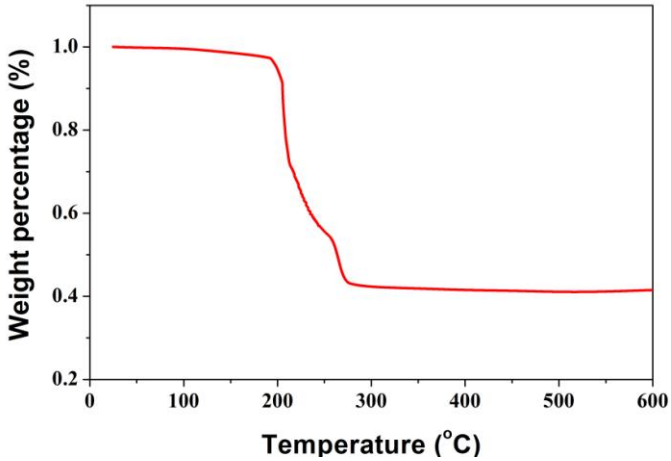

Fig. S15. TGA of cage **1** in air flow (50 mL/min) with temperature ramping rate of 5 ℃/min.

The thermal stability of **1** was investigated using TGA, in the presence of an air flow. As shown in Fig. S15, weight loss from cage **1** takes place in several stages. The first stage occurs below 190 ℃, corresponding to a ca. 3.0 wt% loss. This is assumed to be the result of the release of absorbed moisture from the sample surface. The second stage (ca. 54.0 wt%) occurs in the range 190–280 ℃, possibly arising from the pyrolysis of the organic ligands of cage **1**. From 280 ℃ to 600 ℃, the weight loss only (1.4 wt%), which could be due to some further decomposition of the remaining organic groups.

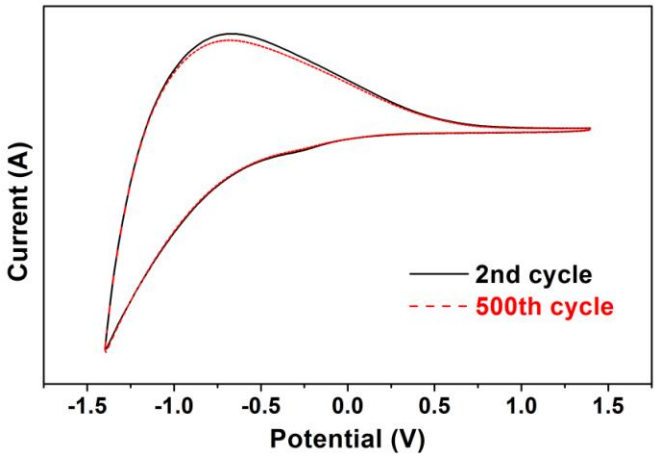

Fig. S16. Long-term stability of **Er@TiO_2-B** film on the ITO electrode as a function of repeated scans in 0.1 M $LiClO_4$/PC solution between -1.4 V and 1.4 V (voltage vs. Ag/AgCl). Scan rate: 100 mV/s.

Fig. S16 presents the stability curves of **Er@TiO_2-B** electrode between -1.4V and 1.4 V for 500 cycles in 0.1 M $LiClO_4$/PC solution. After 500 cycles, the **Er@TiO_2-B** electrode retained 97.4% of its original electroactivity. **Er@TiO_2-B** electrode exhibited higher cycle stability than reported mesoporous spherical TiO_2 electrode, which showed low cycle stability with a retention ratio of 91% after 100 cycles (Ref. 6d). This result implies that **Er@TiO_2-B** electrode has good redox stability and would be a promising candidate material for EC supercapacitor.

Table S6. The optical contrast(ΔT) and switching times for different TiO_2 electrodes.

Electrode	Thickness /nm	ΔT / %	Color time/ s	Bleach time/ s
TiO_2 nanowires	about 350	28.20%	11.3	14.3
TiO_2 nanoparticles	about 350	22.23%	23.7	18.5
Er@TiO_2-B	about 1000	15.26%	16.3	17.7

As shown in Table S6, the optical contrast of **Er@TiO_2-B** electrode was 15.26%, lower than reported[5e] TiO_2 nanowire electrode (28.20%) and TiO_2 nanoparticles electrode (22.23%); while the switching times of Er@TiO_2-B electrode was 16.3 s for coloration and 17.7 s for bleaching, which was

slower than that of TiO_2 nanowire electrode but faster than that of TiO_2 nanoparticles electrode. This phenomenon may be due to the thickness of **Er@TiO_2-B** electrode was much larger than that of TiO_2 nanowires and TiO_2 nanoparticles electrodes.